

Impurity-induced states in superconducting heterostructures

Dong E. Liu,¹ Enrico Rossi,² and Roman M. Lutchyn¹

¹*Station Q, Microsoft Research, Santa Barbara, California 93106-6105, USA*

²*Department of Physics, William & Mary, Williamsburg, VA 23187, USA*

(Dated: November 15, 2017)

Heterostructures allow the realization of electronic states that are difficult to obtain in isolated systems. Exemplary is the case of quasi-one-dimensional heterostructures formed by a superconductor and a semiconductor with spin-orbit coupling in which Majorana zero-energy modes can be realized. We study the effect of a single impurity on the spectrum of superconducting heterostructures. We find that the coupling between the superconductor and the semiconductor can strongly affect the impurity-induced states and may induce additional subgap bound states that are not present in isolated uniform superconductors. For the case of quasi-one-dimensional superconductor/semiconductor heterostructures we obtain the conditions for which the low-energy impurity-induced bound states appear.

Composite heterostructures provide an opportunity to realize states with novel and desirable properties that are different from the individual components. In the last decade, this principle has been implemented very successfully to obtain *composite electronic systems*, heterostructures, with novel and unique electronic properties. For example, the heterostructures combining a conventional s-wave superconductor (SC) and a conductor with strong spin-orbit coupling (SOC) may realize topological superconducting states supporting Majorana zero modes (MZMs)[1–9], and the preliminary signatures of MZMs were observed [10–22]. This example suggests that different heterostructures offer a playground to realize exotic electronic states which are very different from those in the underlying isolated materials.

The presence of impurities in heterostructures, as in any other condensed matter system, is unavoidable. However, their effect on the electronic states can be quite non-trivial due to the interplay between scattering processes involving different materials. The effect of impurities in general varies significantly depending on the component of the heterostructures in which they are located. This fact makes the understanding of impurity effects in heterostructures non trivial and outside the scope of most previous works focusing on impurity effects in single-component homogeneous SC systems [23].

In this work we study the states induced by scalar impurities in heterostructures involving a SC and a semiconductor with Rashba SOC. Our analytical results show that in general the self-energy describing the effect of an isolated impurity consists of two terms that may have opposite signs. We find that the complete or partial cancellation of these two terms is responsible for the presence of low-energy impurity-induced states that are not present in homogeneous SC systems. We find that this cancellation may lead to impurity-induced subgap states even in the limit of vanishing magnetic field. This result does not contradict Anderson’s result [24] given that in our system the superconducting order parameter is not uniform. For the specific case of one-dimensional (1D)

heterostructures formed by a SC and semiconductor with SOC we study how the spectrum of the impurity-induced states changes as a function of an external magnetic field. As shown in Refs. [25–28], a magnetic field may induce a quantum phase transition from a conventional (trivial) superconducting phase to a topological superconducting phase characterized by the presence of MZMs. We identify the regions in parameter space where very low-energy impurity-induced states might affect the observation and manipulation of MZMs.

Theoretical Model. The Hamiltonian H for the heterostructure can be written as $H = H_N + H_{SC} + H_T$, where H_N is the Hamiltonian for the normal, i.e. non-superconducting, component (either a semiconductor or a metal), H_{SC} is the Hamiltonian for the SC and H_T is the term describing tunneling processes between the SC and the normal component. Specifically, H_N and H_{SC} are defined as

$$H_N = \frac{1}{2} \sum_{\mathbf{k}} \psi_{N,\mathbf{k}}^\dagger [\epsilon_{N,\mathbf{k}} \sigma_0 \tau_z + \alpha \mathbf{l}_{\mathbf{k}} \cdot \boldsymbol{\sigma} \tau_z + V_x \sigma_x \tau_z] \psi_{N,\mathbf{k}}, \quad (1)$$

$$H_{SC} = \frac{1}{2} \sum_{\mathbf{k}} \psi_{SC,\mathbf{k}}^\dagger [\epsilon_{SC,\mathbf{k}} \tau_z \sigma_0 - \Delta_0 \tau_y \sigma_y] \psi_{SC,\mathbf{k}}. \quad (2)$$

where $\psi_{\mathbf{k},i}^\dagger = (c_{i,\mathbf{k}\uparrow}^\dagger, c_{i,\mathbf{k}\downarrow}^\dagger, c_{i,-\mathbf{k}\uparrow}, c_{i,-\mathbf{k}\downarrow})$ is the spinor with $i=N$ or $i=SC$, $c_{i,\mathbf{k}\sigma}^\dagger$ ($c_{i,\mathbf{k}\sigma}$) is the creation (annihilation) operator for an electron with momentum \mathbf{k} and spin σ in the i -th part of the heterostructure, $\epsilon_{i,\mathbf{k}} = (\mathbf{k}^2/2m_i - \mu_i)$ with m_i , μ_i the electron’s effective mass and chemical potential, respectively, in the i -th component, σ_j (τ_j) are the Pauli matrices in spin (Nambu) space, α is the strength of the Rashba SO with $\mathbf{l}_{\mathbf{k}} = (k_y, -k_x, 0)$, Δ_0 is the amplitude of the superconducting gap, and V_x is the Zeeman splitting due to the external magnetic field along the x -direction. The tunneling Hamiltonian can be written as

$$H_T = \frac{1}{2} \sum_{\mathbf{k}} \psi_{SC,\mathbf{k}}^\dagger \hat{h}_T(\mathbf{q}) \psi_{N,\mathbf{k}+\mathbf{q}} + h.c. \quad (3)$$

where $\hat{h}_T(\mathbf{q})$ is the tunneling matrix. In our case, assuming that the tunneling processes conserve the spin and the momentum parallel to the SC-N interface (\mathbf{k}_{\parallel}) we have $\hat{h}_T(\mathbf{q}) = t\sigma_0\tau_z\delta(\mathbf{q}_{\parallel})$ with t being the tunneling amplitude. To quantify the effect of the tunneling term it is helpful to introduce the parameter $\Gamma_t \equiv t^2\rho_{F,SC}$, where $\rho_{F,SC}$ is the density of states (DOS) of the SC at the Fermi energy, $E_{F,SC}$.

In the presence of impurities, the Hamiltonian for the system is modified by an additional term, H_{imp} , describing the scattering of electrons off the impurities. For a single isolated impurity located in the i -th ($i = N, SC$) component of the heterostructure

$$H_{\text{imp}} = \sum_{\mathbf{r}} \delta(\mathbf{r}) \psi_{i,\mathbf{r}}^\dagger \hat{h}_{\text{imp}} \psi_{i,\mathbf{r}} = \sum_{\mathbf{k}, \mathbf{k}'} \psi_{i,\mathbf{k}}^\dagger \hat{h}_{\text{imp}} \psi_{i,\mathbf{k}'}. \quad (4)$$

Here $\psi_{i,\mathbf{r}}^\dagger$ ($\psi_{i,\mathbf{r}}$) is the creation (annihilation) operator for an electron at position \mathbf{r} in i -th the component of the heterostructure, and \hat{h}_{imp} is the matrix describing the structure of the impurity in spinor space. For a scalar impurity, using the convention specified above for spinors, we have $\hat{h}_{\text{imp}} = u_{\text{imp}}\sigma_0\tau_z$ where u_{imp} is the strength of the impurity potential.

The spectrum of the impurity-induced states can be obtained by locating the poles of the T matrix [29]. Using the diagrammatic approach, one can express the T -matrix in terms of the Green's function for the isolated components of the heterostructure $G_i^{(0)}(\mathbf{k}, \omega) = (\omega + i\eta - H_i)^{-1}$ with $i = N, SC$. If the impurity is located in the i -th component of the heterostructure the matrix, T_i , is given by

$$T_i(\omega) = \left[\mathbb{1} - \hat{h}_{\text{imp}} \Sigma_{i,\text{imp}}(\omega) \right]^{-1} \hat{h}_{\text{imp}}, \quad (5)$$

where $\Sigma_{i,\text{imp}}(\omega) = \int d\mathbf{k} G_i(\mathbf{k}, \omega)$ and $G_i(\mathbf{k}, \omega)$ is the Green's function of the i -th component of the heterostructure *dressed* by the self-energy $\Sigma_{i,t}(\mathbf{k}_{\parallel}, \omega)$ due to the tunneling term:

$$G_i(\mathbf{k}, \omega) = \left[(G_i^{(0)}(\mathbf{k}, \omega))^{-1} - \Sigma_{i,t}(\mathbf{k}, \omega) \right]^{-1} \quad (6)$$

$$\Sigma_{i,t}(\mathbf{k}, \omega) = \int d\mathbf{q} \hat{h}_T(\mathbf{q}) G_i^{(0)}(\mathbf{k} + \mathbf{q}, \omega) \hat{h}_T(-\mathbf{q}). \quad (7)$$

Here $G_i^{(0)}$ is the Green's function of the heterostructure's component coupled via the tunneling term to the i -th component. Using Eq.(3), we obtain

$$\Sigma_{i,t}(\mathbf{k}_{\parallel}, \omega) = t^2 \int d\mathbf{q}_{\perp} \sigma_0 \tau_z G_i^{(0)}(\mathbf{k}_{\parallel}, \mathbf{q}_{\perp}, \omega) \sigma_0 \tau_z. \quad (8)$$

To understand how the presence of the tunneling term affects the spectrum of the impurity-induced states it is useful to express T_i in the following equivalent form:

$$T_i = \left[\mathbb{1} - \hat{h}_{\text{imp}} \left(\Sigma_{i,\text{imp}}^{(0)}(\omega) + \Sigma_{i,\text{imp}}^{(1)}(\omega) \right) \right]^{-1} \hat{h}_{\text{imp}} \quad (9)$$

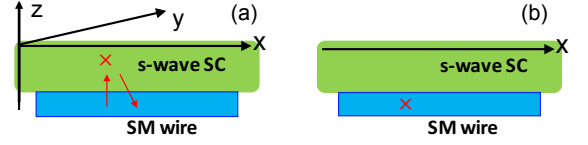


FIG. 1. (Color online) Sketch of 1D superconductor/semiconductor heterostructure with an isolated impurity in the SC (a) and semiconductor (N) (b).

where

$$\Sigma_{i,\text{imp}}^{(0)}(\omega) = \int d\mathbf{k} G_i^{(0)}(\mathbf{k}, \omega), \quad (10)$$

$$\Sigma_{i,\text{imp}}^{(1)}(\omega) = \int d\mathbf{k} G_i^{(0)}(\mathbf{k}, \omega) \Sigma_{i,t}(\mathbf{k}, \omega) G_i(\mathbf{k}, \omega). \quad (11)$$

As follows from above, there are two contributions that determine the pole structure of T_i : $\Sigma_{i,\text{imp}}^{(0)}$ the term that appears if the component i were isolated, and $\Sigma_{i,\text{imp}}^{(1)}(\omega)$ the term due to tunneling processes between the i -th and \bar{i} -th component of the heterostructure. If tunneling is not a weak perturbation, the interplay between these two terms may lead to unusual properties for the spectrum of impurity-induced states in heterostructures.

For the case when the impurity is located in the normal component (in the remainder we assume it to be a semiconductor) the effect of the tunneling term is to induce a SC gap in it (Δ_{ind}) and is straightforward from Eq. (5) to obtain $T_N(\omega) = [\tau_z\sigma_0 - u_{\text{imp}}\hat{\Sigma}_{N,\text{imp}}(\omega)]^{-1}u_{\text{imp}}$. When no SOC is present ($\alpha = 0$), $T_N(\omega)$ does not have poles ω^* below the induced gap (i.e. $|\omega^*| \geq \Delta_{\text{ind}}$). In the presence of SOC in the semiconductor the superconducting pairing will mix spin-singlet and spin-triplet pairing components, even though in the SC only s-wave pairing is present [30–32]. In this situation T_N may have poles for $|\omega| < \Delta_{\text{ind}}$. To further investigate this case we consider the quasi-1D system shown in Fig. 1 in which L_y, L_z are finite and $L_x \rightarrow \infty$ and the spectrum of the system consist of well separated 1D subbands ϵ_{k_x} . For concreteness in the remainder we limit ourselves to the case in which only one spinful subband is occupied. When V_x is larger than a critical value, V_x^c , the system is expected to be in a topological phase [27, 28]. For parameter values relevant for current experiments [29] for $V_x < V_x^c$ the impurity-induced states have energies, ω^* , very close to the induced-gap edge. When the chemical potential is much larger than SC bulk gap [29], in the trivial regime, $|\omega^*|$ can be smaller than Δ_{ind} , albeit it does not approaches zero. The spectrum of the impurity-induced states is completely different in the topological regime. In this regime the induced superconducting pairing is p-wave and we find that the energy of the bound states: (i) depends very strongly on u_{imp} , (ii) it is strongly asymmetric with respect to $u_{\text{imp}} = 0$, (iii) it can go to zero for finite (negative) values of u_{imp} [33]. This can be seen in Fig. 2 (a) where the dependence of ω^* on $u_{\text{imp}}\rho_F$ (ρ_F be

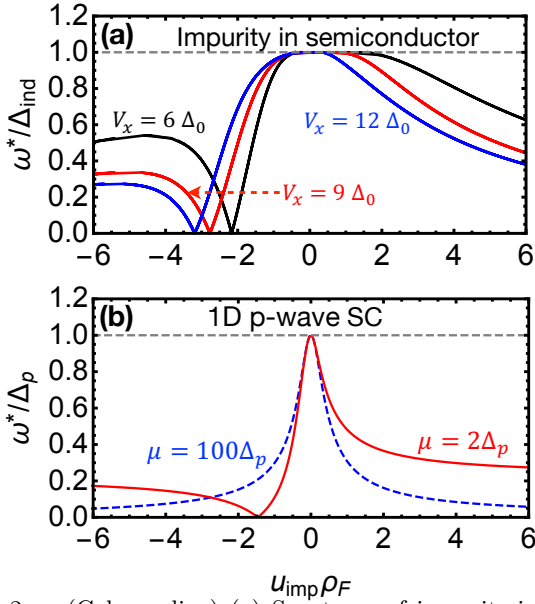


FIG. 2. (Color online) (a) Spectrum of impurity-induced bound states for 1D SM/SC heterostructure as a function of $u_{\text{imp}}\rho_F$ for the case (a) of Fig.1 and $V_x > V_x^c$. Here $\hbar^2 k_{F,N}^2/(2m_N) = 1.5\Delta_0$, $\alpha_{SO}k_{F,N} = 4.2\Delta_0$, $\mu = 1.5\Delta_0$, $\Gamma_t = 5\Delta_0$, $V_x^c \approx 5.2\Delta_0$ (see Ref. [29] for more details). (b) Spectrum of impurity-induced bound state for a 1D p-wave SC as a function $u_{\text{imp}}\rho_F$ for different values of μ .

ing the DOS of the semiconductor (N) at ϵ_F) for different values of the Zeeman splitting $V_x > V_x^c$.

The results shown in Fig. 2 (a) can be qualitatively understood considering a scalar impurity, Eq. (4), in a 1D p-wave superconductor for which: $H_{\text{pSC}} = \sum_{k_x, \sigma, \sigma'} [c_{k_x, \sigma}^\dagger (k_x^2/2m - \mu) \sigma_0 c_{k_x, \sigma'} + i\Delta_p (k_x/k_F) c_{k_x, \sigma}^\dagger \mathbf{d}_{k_x} \cdot \boldsymbol{\sigma} \sigma_y c_{-k_x, \sigma'}^\dagger + \text{h.c.}]$, where $\Delta_p(k_x/k_F) = -\Delta_p(-k_x/k_F)$ is the amplitude of the superconducting p-wave pairing and \mathbf{d}_{k_x} is the unit vector characterizing the polarization of the triplet state [34]. In this case $T(\omega) = u_{\text{imp}}[\tau_z - u_{\text{imp}} \int dk_x G_{\text{p-SC}}(\omega, k_x)]^{-1}$, where $G_{\text{p-SC}}(\omega, k_x) = (\omega + i\eta - H_{\text{p-SC}})^{-1}$. Due to the 1D nature of the carriers, one finds that, at low energies, the density of states is strongly dependent on their energy ϵ : $\rho(\epsilon) \approx 1/\sqrt{|\epsilon|}$. This fact makes the energy of the impurity bound state strongly dependent on u_{imp} when the Fermi energy ($E_{F,N}$) is close to the bottom of the band. This is shown in Fig. 2 (b) where we can see that the energy of the bound state depends strongly on u_{imp} when μ is small (solid line) and fairly weakly for large μ (dashed line) [35]. We should emphasize that this asymmetry effect is very relevant for 1D topological SC wires supporting MZMs in which typically μ must be quite small, i.e. $|\mu| < \sqrt{V_x^2 - \Delta_{\text{ind}}^2}$ [25–28].

In the most recent realizations of 1D topological SC wires [9, 19–21] the semiconductor and the interface between the semiconductor and the SC are of very high quality so that very few impurities are expected to be present in the semiconductor or at the interface. On the other hand, the SC (i.e. aluminum) is disordered.

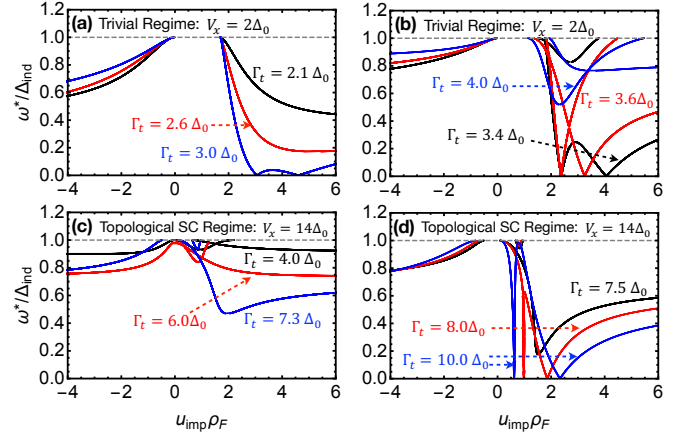


FIG. 3. (Color online) Spectrum of impurity-induced bound states as function of $u_{\text{imp}}\rho_F$ for 1D SM/SC heterostructure when the impurity is located in the SC in the trivial regime, (a) and (b), and topological regime (c) and (d). Here $\hbar^2 k_{F,N}^2/(2m_N) = 1.5\Delta_0$, $\mu = 1.5\Delta_0$, $\alpha_{SO}k_{F,N} = 4.2\Delta_0$, $k_{F,N}/k_{F,SC} = 0.3$ (see [29] for details).

Therefore, henceforth we consider the situation in which the impurities are located in the SC. In this case, using Eq. (9) one finds

$$T_{\text{SC}} = \frac{u_{\text{imp}}}{\tau_z \sigma_0 - u_{\text{imp}} \Sigma_{\text{SC,imp}}^{(0)}(\omega) - u_{\text{imp}} \Sigma_{\text{SC,imp}}^{(1)}(\omega)}. \quad (12)$$

For the case in which the SC is s-wave and the tunneling is such that $\hat{h}_T = t\delta(\mathbf{q})\sigma_z\tau_0$ we obtain

$$\Sigma_{\text{SC,imp}}^{(0)}(\omega) = -\frac{\rho_{\text{SC}}}{\sqrt{\Delta_0^2 - \omega^2}} [\omega\sigma_0\tau_0 + \Delta_0\sigma_y\tau_y] \quad (13)$$

$$\Sigma_{\text{SC,imp}}^{(1)}(\omega) = \int d\mathbf{k}_{\parallel} \int d\mathbf{k}_{\perp} G_{\text{SC}}^{(0)}(\mathbf{k}_{\parallel}, \mathbf{k}_{\perp}, \omega) \Sigma_{\text{SC,t}}(\mathbf{k}_{\parallel}, \omega) G_{\text{SC}}(\mathbf{k}_{\parallel}, \mathbf{k}_{\perp}, \omega) \quad (14)$$

with $\Sigma_{\text{SC,t}}(\mathbf{k}_{\parallel}, \omega)$ given by Eq. (7). One can show that the strength of the second term $\Sigma_{\text{SC,imp}}^{(1)}(\omega)$ is proportional to the dimensionless parameter $\alpha_{\text{SW}} = \frac{\Gamma_t}{E_{F,N}} \frac{k_{F,N}}{k_{F,SC}}$ (see [29] for details) where $k_{F,N}$, $k_{F,SC}$ are the Fermi momenta in the SM and SC, respectively.

Fig. 3 (a) shows the spectrum of the impurity-induced states as a function of $u_{\text{imp}}\rho_F$ (where now $\rho_F = \rho_{F,SC}$) for the 1D case in which the SM/SC heterostructure is in the topologically trivial phase, $V_x = 2\Delta_0 < V_x^c$, and different values of Γ_t . In the limit $\alpha_{\text{SW}} \rightarrow 0$, $t \neq 0$ (i.e. $\Sigma_{\text{SC,imp}}^{(1)} \rightarrow 0$ and $\Delta_{\text{ind}} \neq 0$), we find bound states close to the gap edge. As α_{SW} increases, the interplay between $\Sigma_{\text{SC,imp}}^{(0)}$ and $\Sigma_{\text{SC,imp}}^{(1)}$ may lead to low-lying subgap states as demonstrated in Figs. 3 (a) and (b). The results of Fig. 3 (b) also show that as Γ_t increases the spectrum of the impurity-induced bound states becomes more asymmetric with respect to $u_{\text{imp}}\rho_F$ as we have found for the case in which the impurity is located in the SM. It is

very interesting to notice that, contrary to the case when an impurity is located in the SM, shown in Figs. 2 (a) and (b), an impurity in SC may lead to low-lying subgap states with $\omega^* \rightarrow 0$ in the trivial regime.

Figs. 3 (c), (d) show the results when the SM/SC heterostructure is in the topological phase $V_x = 14\Delta_0 > V_x^{(c)}$. One can see that the spectrum is strongly asymmetric in this case even for relatively small values of Γ_t , Figs. 3 (c). For larger Γ_t we find that also in the topological phase the impurity can induce zero energy bound states for relatively small values of $u_{\text{imp}}\rho_F$, Figs. 3 (d). These results suggest that in the topological phase the value of u_{imp} necessary to induce a zero-energy bound state decreases as Γ_t increases. Thus, there is an optimal value of Γ_t for which the induced gap is large and, at the same time, impurities in SC do not result in significant subgap density of states.

The spectrum of the impurity bound states as a function of Zeeman coupling for $V_x < V_x^{(c)}$ and fixed Γ_t is shown in Fig. 4 (a). As one can see there is a threshold value of V_x for the emergence of low-energy bound states with $\omega^* \rightarrow 0$. We plot the value of $|u_{\text{imp}}^*\rho_F|$ such that $\omega^* = 0$ as a function of V_x in Fig. 4 (b): one of the solutions decreases and approaches to a constant value at topological transition whereas the other one increases to infinity. Similarly, we study the topological SC regime in Figs. 4 (c), (d). As we increase V_x , two zero-energy solutions merge and then disappear.

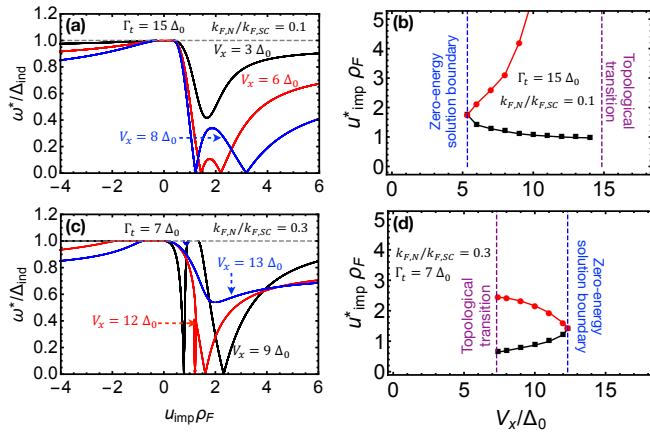


FIG. 4. (Color online) Evolution of impurity-induced bound spectrum with Zeeman field for trivial regime (a), (b) with $V_x < V_x^{(c)}$ and fixed $\Gamma_t = 15\Delta_0$, $k_{F,N}/k_{F,SC} = 0.1$, and topological SC regime (c), (d) with $V_x > V_x^{(c)}$ and fixed $\Gamma_t = 7\Delta_0$, $k_{F,N}/k_{F,SC} = 0.3$. (a) and (c) impurity-induced bound spectrum for several values of V_x . (b) and (d) Two zero-energy solutions (black squares and red dots) $|u_{\text{imp}}^*\rho_F|$ as a function of V_x . The vertical dashed lines denote the topological phase transition (purple) and the boundaries with zero-energy solutions (blue) shown in Fig. 5.

Considering that V_x and Γ_t are two of the key parameters that can be controlled in experiments to real-

ize MZMs in proximitized nanowires, the knowledge of where in the (V_x, Γ_t) plane $\omega^* = 0$ is of great importance for the realization of topological qubits based on such systems [36–39]. Figs. 5 (a), (b) show in grey-blue the regions (with black solid boundaries) in the (V_x, Γ_t) plane for which there exist a finite value of u_{imp} such that $\omega^* = 0$. The red dashed line shows the boundary between trivial and topological regimes. The blue dot-dashed line identifies the regions (yellow) for which a finite value of u_{imp} exists such that $\omega^* < 0.6\Delta_{\text{ind}}$, these regions, of course, contain the grey-blue regions where $\omega^* = 0$. The horizontal dashed line in Fig. 5 (a) (Fig. 5 (b)) identifies the value of Γ_t for which the results of Fig. 4 (a), (b) (Fig. 4 (c), (d)) were obtained. As follows from Fig. 5 (a), the area where $\omega^* = 0$ is rather large in the trivial regime and becomes smaller in the topological one when $k_{F,N}/k_{F,SC} \ll 1$. Thus, the ratio of $k_{F,N}/k_{F,SC}$ is an important parameter when optimizing superconducting materials. For aluminum-based proximitized nanowires this parameter is quite small, $k_{F,N}/k_{F,SC} \ll 1$. The parameter α_{SWS} can be controlled experimentally by changing the back-gate voltage in proximitized nanowires [40] so the propensity for the formation of impurity-induced bound states we predict, see Fig. 5, can be tested experimentally.

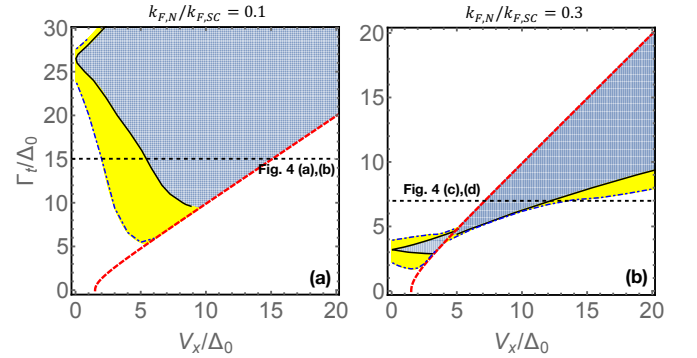


FIG. 5. (Color online) Phase diagram in (V_x, Γ_t) plane identifying the regions, shown in grey-blue (dark in grey-scale) with solid line boundaries, for which the existence of $\omega^* = 0$ solution for some finite value of u_{imp} , and $\frac{\hbar^2 k_{F,N}^2}{2m_N} = 1.5\Delta_0$, $\mu = 1.5\Delta_0$, $\alpha_{SO}k_{F,N} = 4.2\Delta_0$. The red dashed line shows the boundary between trivial and topological regime. The blue dot-dashed lines identified the boundaries of the yellow (light in grey-scale) regions where $\omega^* < 0.6\Delta_{\text{ind}}$. The horizontal dash line in (a) and (b) is placed at the value of Γ_t for which the results of Fig. 4 were obtained.

Conclusions. We have studied impurity-induced subgap states in superconductor-based heterostructures. In the case of proximitized nanowires, considered in this work in details, we find that in these structures there is a large region in parameter space for which the impurities in the superconductor can induce low energy states even when the superconductor is purely s-wave.

Our work presents results for the spectrum of the bound states induced by a single impurity and so is complementary to the previous studies that considered the case of many-impurities [41–50] via disorder-averaging techniques. Our results are directly relevant to experimental situations in which the impurity density is low and disorder-averaging is not justified. In addition, they are

instrumental to extend the study of the effect of many-impurities via disorder-averaging to the unitarity limit, i.e. the limit of strong impurities, both for the case when the impurities are located in the semiconductor and the case when they are located in the superconductor.

Acknowledgments. ER acknowledges support from NSF CAREER DMR-1455233, ARO-W911NF-16-1-0387, and ONR-N00014-16-1-3158.

Supplementary Information for “Impurity-induced states in superconducting heterostructures”

In this supplementary material we provide: (i) details on the derivation of the T-matrix expression for the case when the impurity is located in the superconductor, see Eq. (13-15) of the main text, (ii) the relation between the parameters values used in our calculations to the parameters values of current experiments on quasi 1D SM-SC heterostructures, (iii) the spectrum of the impurity-induced states for the case when the impurity is located in the SM and the chemical potential in the SM is much larger than the SC’s gap.

T-matrix calculation for an impurity in the superconductor

The scattering T-matrix for a single impurity in a superconductor proximity-coupled to a semiconductor nanowire can be described by a diagrammatic representation shown in Fig. 6:

$$\begin{aligned}
T_{SC}(\omega) &= u_{imp}\tau_z\sigma_0 + u_{imp}^2\tau_z\sigma_0 \cdot \left(\Sigma_{SC,imp}^{(0)}(\omega) + \Sigma_{SC,imp}^{(1)}(\omega) \right) \cdot \tau_z\sigma_0 \\
&\quad + u_{imp}^3\tau_z\sigma_0 \cdot \left(\Sigma_{SC,imp}^{(0)}(\omega) + \Sigma_{SC,imp}^{(1)}(\omega) \right) \cdot \tau_z\sigma_0 \cdot \left(\Sigma_{SC,imp}^{(0)}(\omega) + \Sigma_{SC,imp}^{(1)}(\omega) \right) \cdot \tau_z\sigma_0 + \dots \\
&= \frac{u_{imp}}{\tau_z\sigma_0 - u_{imp}\Sigma_{SC,imp}^{(0)}(\omega) - u_{imp}\Sigma_{SC,imp}^{(1)}(\omega)}, \tag{15}
\end{aligned}$$

where $\Sigma_{SC,imp}^{(0)}(\omega)$ represents the contribution to the self-energy for a clean s-wave superconductor:

$$\Sigma_{SC,imp}^{(0)}(\omega) = \sum_{\vec{k}} G_{SC}^{(0)}(\omega, \vec{k}) = \rho_{SC} g^{qc}(\omega) = -\frac{\rho_{SC}}{\sqrt{\Delta_0^2 - \omega^2}} \begin{pmatrix} \omega\sigma_0 & (\Delta_0 i\sigma_y)^\dagger \\ (\Delta_0 i\sigma_y) & \omega\sigma_0 \end{pmatrix}. \tag{16}$$

$$\begin{aligned}
T_{SC}(\omega) &= \begin{array}{c} \text{X} \\ | \\ | \\ | \end{array} + \begin{array}{c} \text{X} \quad \text{X} \\ | \quad | \\ \text{---} \quad \text{---} \\ | \quad | \\ \rho_F \Sigma_{SC,imp}^{(0)}(\omega) \end{array} + \begin{array}{c} \text{X} \quad \text{X} \\ | \quad | \\ \text{---} \quad \text{---} \\ | \quad | \\ \rho_F \Sigma_{SC,imp}^{(1)}(\omega) \end{array} + \begin{array}{c} \text{X} \quad \text{X} \quad \text{X} \\ | \quad | \quad | \\ \text{---} \quad \text{---} \quad \text{---} \\ | \quad | \quad | \end{array} + \begin{array}{c} \text{X} \quad \text{X} \quad \text{X} \\ | \quad | \quad | \\ \text{---} \quad \text{---} \quad \text{---} \\ | \quad | \quad | \end{array} + \begin{array}{c} \text{X} \quad \text{X} \quad \text{X} \\ | \quad | \quad | \\ \text{---} \quad \text{---} \quad \text{---} \\ | \quad | \quad | \end{array} + \begin{array}{c} \text{X} \quad \text{X} \quad \text{X} \\ | \quad | \quad | \\ \text{---} \quad \text{---} \quad \text{---} \\ | \quad | \quad | \end{array} + \dots
\end{aligned}$$

FIG. 6. Diagrammatic representation of the scattering T-matrix for a single impurity in the superconductor of the superconducting heterostructure. The scattering involving two scatterings have two events: 1) scatterings only in s-wave SC, 2) scatterings where electrons travel through the SM. The double solid line (red): propagator in s-wave SC; the dashed-solid line (black): propagator in semiconductor wire with proximity induced SC; the cross head - dashed line represents the impurity scattering.

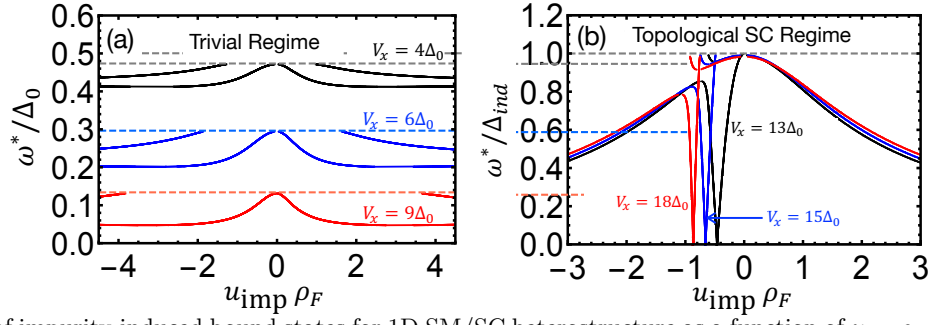


FIG. 7. Spectrum of impurity-induced bound states for 1D SM/SC heterostructure as a function of $u_{\text{imp}}\rho_F$ for the case in which the impurity is in the semiconductor. $k_{F,N}^2/(2m_w) = 10\Delta_0$, $\alpha k_F = 3\Delta_0$, $\Gamma_t = 5\Delta_0$ in the trivial regime, (a), and topological regime (b). Here the topological transition occurs at $V_x^c \approx 11.2\Delta_0$

Above expression corresponds to Eq. (14) of the main text. The second term $\Sigma_{SC,imp}^{(1)}(\omega)$ represents a process of an electron tunneling between the SC and semiconductor nanowire and scattering off the impurity

$$\Sigma_{SC,imp}^{(1)}(\omega) = \int d\mathbf{k}_{\parallel} d\mathbf{k}_{1,\perp} d\mathbf{k}_{2,\perp} G_{SC}^{(0)}(\mathbf{k}_{\parallel}, \mathbf{k}_{1,\perp}, \omega) \Sigma_{SC,t}(\mathbf{k}_{\parallel}, \omega) G_{SC}(\mathbf{k}_{\parallel}, \mathbf{k}_{2,\perp}, \omega), \quad (17)$$

$$= t^2 \int d\mathbf{k}_{\parallel} d\mathbf{k}_{1,\perp} d\mathbf{k}_{2,\perp} G_{SC}^{(0)}(\mathbf{k}_{\parallel}, \mathbf{k}_{1,\perp}, \omega) \cdot \tau_z \sigma_0 \cdot G_N(\mathbf{k}_{\parallel}, \omega) \cdot \tau_z \sigma_0 \cdot G_{SC}^{(0)}(\mathbf{k}_{\parallel}, \mathbf{k}_{2,\perp}, \omega). \quad (18)$$

Here t is tunneling matrix element between the SC and nanowire (N), G_N is the dressed semiconductor Green function (in proximity to a clean SC). We assume that momentum parallel to the SC-N interface is conserved.

The largest contribution to the scattering in SC comes from on-shell processes (i.e. close to the Fermi surface). Therefore, it's convenient to introduce $\delta\mathbf{k} \equiv (\delta k, \hat{\Omega})$, where $\delta k = |\mathbf{k} - \mathbf{k}_{F,SC}| \ll k_{F,SC}$ and $\hat{\Omega} \equiv \mathbf{k}/|\mathbf{k}|$. One can approximate the quasiparticle energy spectrum in the superconductor $\epsilon(k)$ as $\epsilon(k) = v_{F,SC}\delta k$ where $v_{F,SC}$ is the Fermi velocity in the superconductor. After integration over k , the bulk Green's function in the SC, $G_{SC}^{(0)}$, becomes almost independent of the momentum $\hat{\Omega}$. Since the integral over k mostly comes from the contribution of pole near Fermi energy, one can perform the integration over k analytically:

$$\Sigma_{SC,imp}^{(1)}(\omega) = \frac{L_z k_{F,N}}{E_{F,N}} t^2 \int d\hat{\Omega} \left(\frac{\rho_{SC}}{k_{F,SC} L_z} \int d\delta k G_{SC}(\omega; \delta k, \hat{\Omega}) \right) \cdot \tau_z \sigma_0 \cdot R(\omega) \cdot \tau_z \sigma_0 \cdot \int d\hat{\Omega} \left(\frac{\rho_{SC}}{k_{F,SC} L_z} \int d\delta k G_{SC}(\omega; \delta k, \hat{\Omega}) \right), \quad (19)$$

where $k_{F,N}$ and $E_{F,N}$ are the Fermi wavevector and Fermi energy in the semiconductor wire, respectively, ρ_{SC} the normal-state density of states (DOS) of the SC, and

$$R(\omega) \equiv E_{F,N} \int \frac{d\tilde{\mathbf{k}}_{\parallel}}{2\pi} G_N(\omega; \tilde{\mathbf{k}}_{\parallel}) \text{ with } \tilde{\mathbf{k}}_{\parallel} = \frac{\mathbf{k}_{\parallel}}{k_{F,N}}. \quad (20)$$

Notice that the DOS contributing to the N-SC tunneling amplitude is given by $\rho_{SC}^t = \rho_{SC}/(k_{F,SC} L_z)$. Assuming the bare SC Green's function $G_{SC}(\omega; k, \hat{\Omega})$ to be isotropic and, thus, independent of $\hat{\Omega}$, one can simplify the expression for $\Sigma_{SC,imp}^{(1)}(\omega)$:

$$\Sigma_{SC,imp}^{(1)}(\omega) = \alpha_{swS} \rho_{SC} [g^{qc}(\omega) \cdot \tau_z \sigma_0 \cdot R(\omega) \cdot \tau_z \sigma_0 \cdot g^{qc}(\omega)] \quad (21)$$

where the dimensionless parameter α_{swS} reads

$$\alpha_{swS} = \frac{\Gamma_t}{E_{F,N}} \frac{k_{F,N}}{k_{F,SC}} \text{ where } \Gamma_t = \pi |t|^2 \rho_{SC}^t. \quad (22)$$

Notice that the presence of the vertex matrix $\tau_z \sigma_0$ flips the position of the zero energy solutions from $u_{\text{imp}}^* \rho_F < 0$ to $u_{\text{imp}}^* \rho_F > 0$ (please compare Fig. 2 with Fig. 3 and 4 in the main text).

Parameters used in the calculation vs Experimental values

Here, we briefly explain how to choose the numerical parameters based on relevant experimental systems [2–5, 9]. We consider aluminum/InSb (SC/N), and choose for the superconducting gap of the bulk SC $\Delta_0 = 0.2meV$, effective mass of the semiconductor (N) $m_{\text{eff}} = 0.014m_e$ with m_e the electron's mass, and the Rashba spin-orbit coupling strength of semiconductor $\alpha_{SO} = 0.2 - 1eV \cdot \text{\AA}$. We consider the energy dispersion of semiconductor wire (without Rashba spin-orbit coupling and Zeeman splitting) as $\epsilon_{N,k} = \frac{\hbar k^2}{2m_{\text{eff}}} - \mu = \frac{\hbar k_{F,N}^2}{2m_{\text{eff}}} (\hat{k}^2 - 1)$ with $\hat{k} = k/k_{F,N}$. Including both Rashba coupling and Zeeman splitting, the energy spectrum $E_N(\hat{k}) = \frac{\hbar k_{F,N}^2}{2m_{\text{eff}}} (\hat{k}^2 - 1) \pm \sqrt{V_x^2 + (\hat{k}k_{F,N}\alpha_{SO})^2}$ with the Fermi surface corresponding to $E_N(\hat{k}^*) = 0$, and so the Rashba spin-orbit energy can be written as $E_{SO} = \hat{k}^*k_{F,N}\alpha_{SO}$. In the numerical calculation of the main text, we fixed the parameters $\Delta_0 = 0.2meV$, $m_{\text{eff}} = 0.014m_e$, $\alpha_{SO} = 0.8eV \cdot \text{\AA}$. We choose $\frac{\hbar k_{F,N}^2}{2m_{\text{eff}}} = 1.5\Delta_0$, from which we get $k_{F,N}\alpha_{SO} = 4.22\Delta_0$.

Bound states for Impurity in the semiconductor: topological trivial regime

In this section, we consider impurity in the semiconductor, and show that interesting bound states appears even in the topological trivial regime, if the chemical potential is large. Here, rather than those with smaller chemical potential in the main text, we choose a different parameter set: $\Delta_0 = 0.2meV$, $m_{\text{eff}} = 0.014m_e$, $\alpha_{SO} = 0.22eV \cdot \text{\AA}$. We choose $\frac{\hbar k_{F,N}^2}{2m_{\text{eff}}} = 10.0\Delta_0$, from which we get $k_{F,N}\alpha_{SO} = 3.0\Delta_0$. Fig. 7 (a) and (b) show how ω^* depends on $u_{\text{imp}}\rho_F$, where ρ_F is the DOS of the semiconductor (N) at the Fermi energy, for different values of the Zeeman splitting V_x . The top (middle) panel shows the results for $V_x < V_x^c$ ($V_x > V_x^c$), the dashed lines show the value of Δ_{ind} . Interestingly, we can see that the impurity bound states (non-zero energy) could appear within the induced-gap even for the topological trivial regime. We also notice that the bound states shift to the induced-gap edge if we decrease the parameter $\frac{\hbar k_{F,N}^2}{2m_{\text{eff}}}$, for an example $\frac{\hbar k_{F,N}^2}{2m_{\text{eff}}} = 1.5\Delta_0$ considered in the main text. We see that in the trivial regime the energy of the impurity-induced states becomes smaller as V_x increases but it never goes to zero. We also notice that the energy of the bound states depends weakly on u_{imp} with a slight asymmetry of the spectrum with respect to the sign of the potential of the impurity.

-
- [1] M. Z. Hasan and C. L. Kane, *Reviews of Modern Physics* **82**, 3045 (2010), arXiv:1002.3895 [cond-mat.mes-hall].
- [2] C. W. J. Beenakker, *Annu. Rev. Condens. Matter Phys.* **4**, 113 (2013), arXiv:1112.1950.
- [3] J. Alicea, *Reports on Progress in Physics* **75**, 076501 (2012), arXiv:1202.1293.
- [4] M. Leijnse and K. Flensberg, *Semiconductor Science Technology* **27**, 124003 (2012), arXiv:1206.1736.
- [5] T. D. Stanescu and S. Tewari, *Journal of Physics Condensed Matter* **25**, 233201 (2013), arXiv:1302.5433.
- [6] S. R. Elliott and M. Franz, *Rev. Mod. Phys.* **87**, 137 (2015).
- [7] S. Das Sarma, M. Freedman, and C. Nayak, *npj Quantum Information* **1** (2015), arXiv:1501.02813.
- [8] M. Sato and S. Fujimoto, *Journal of the Physical Society of Japan* **85**, 072001 (2016), <http://dx.doi.org/10.7566/JPSJ.85.072001>.
- [9] R. M. Lutchyn, E. P. A. M. Bakkers, L. P. Kouwenhoven, P. Krogstrup, C. M. Marcus, and Y. Oreg, ArXiv e-prints (2017), arXiv:1707.04899 [cond-mat.supr-con].
- [10] V. Mourik, K. Zuo, S. M. Frolov, S. R. Plissard, E. P. A. M. Bakkers, and L. P. Kouwenhoven, *Science* **336**, 1003 (2012), arXiv:1204.2792.
- [11] L. P. Rokhinson, X. Liu, and J. K. Furdyna, *Nat. Phys.* **8**, 795 (2012), arXiv:1204.4212.
- [12] M. T. Deng, C. L. Yu, G. Y. Huang, M. Larsson, P. Caroff, and H. Q. Xu, *Nano Letters* **12**, 6414 (2012), arXiv:1204.4130.
- [13] H. O. H. Churchill, V. Fatemi, K. Grove-Rasmussen, M. T. Deng, P. Caroff, H. Q. Xu, and C. M. Marcus, *Phys. Rev. B* **87**, 241401 (2013), arXiv:1303.2407.
- [14] A. Das, Y. Ronen, Y. Most, Y. Oreg, M. Heiblum, and H. Shtrikman, *Nat. Phys.* **8**, 887 (2012), arXiv:1205.7073.
- [15] A. D. K. Finck, D. J. Van Harlingen, P. K. Mohseni, K. Jung, and X. Li, *Phys. Rev. Lett.* **110**, 126406 (2013).
- [16] S. Nadj-Perge, I. K. Drozdov, J. Li, H. Chen, S. Jeon, J. Seo, A. H. MacDonald, B. A. Bernevig, and A. Yazdani, *Science* **346**, 602 (2014), arXiv:1410.0682.
- [17] M. T. Deng, C. L. Yu, G. Y. Huang, M. Larsson, P. Caroff, and H. Q. Xu, *Scientific Reports* **4**, 7261 (2014).
- [18] A. P. Higginbotham, S. M. Albrecht, G. Kirsanskas, W. Chang, F. Kuemmeth, P. Krogstrup, T. S. Jespersen, J. Nygard, K. Flensberg, and C. M. Marcus, *Nature Physics* **11**, 1017 (2015), arXiv:1501.05155.
- [19] S. M. Albrecht, A. P. Higginbotham, M. Madsen, F. Kuemmeth, T. S. Jespersen, J. Nygård, P. Krogstrup, and C. M. Marcus, *Nature (London)* **531**, 206 (2016), arXiv:1603.03217.
- [20] M. T. Deng, S. Vaitiekėnas, E. B. Hansen, J. Danon, M. Leijnse, K. Flensberg, J. Nygård, P. Krogstrup, and C. M. Marcus, *Science* **354**, 1557 (2016).

- [21] H. Zhang, Ö. Gül, S. Conesa-Boj, K. Zuo, V. Mourik, F. K. de Vries, J. van Veen, D. J. van Woerkom, M. P. Nowak, M. Wimmer, D. Car, S. Plissard, E. P. A. M. Bakkers, M. Quintero-Pérez, S. Goswami, K. Watanabe, T. Taniguchi, and L. P. Kouwenhoven, “Ballistic Majorana nanowire devices,” (2016), [arXiv:1603.04069](#).
- [22] H. Zhang, C.-X. Liu, S. Gazibegovic, D. Xu, J. A. Logan, G. Wang, N. van Loo, J. D. Bommer, M. W. de Moor, D. Car, R. L. M. O. het Veld, P. J. van Veldhoven, S. Koelling, M. A. Verheijen, M. Pendharkar, D. J. Pennachio, B. Shojaei, J. S. Lee, C. J. Palmstrom, E. P. Bakkers, S. Das Sarma, and L. P. Kouwenhoven, (2017), [arXiv:1710.10701](#).
- [23] A. V. Balatsky, I. Vekhter, and J.-X. Zhu, *Reviews of Modern Physics* **78**, 373 (2006).
- [24] P. W. Anderson, *Journal of Physics and Chemistry of Solids* **11**, 26 (1959).
- [25] J. D. Sau, R. M. Lutchyn, S. Tewari, and S. D. Sarma, *Phys. Rev. Lett.* **104**, 040502 (2010).
- [26] J. Alicea, *Phys. Rev. B* **81**, 125318 (2010).
- [27] R. M. Lutchyn, J. D. Sau, and S. Das Sarma, *Phys. Rev. Lett.* **105**, 077001 (2010), [arXiv:1002.4033](#).
- [28] Y. Oreg, G. Refael, and F. von Oppen, *Phys. Rev. Lett.* **105**, 177002 (2010), [arXiv:1003.1145](#).
- [29] Supplementary Material Document.
- [30] L. P. Gor’kov and E. I. Rashba, *Phys. Rev. Lett.* **87**, 037004 (2001).
- [31] P. A. Frigeri, D. F. Agterberg, A. Koga, and M. Sigrist, *Phys. Rev. Lett.* **92**, 097001 (2004).
- [32] C. Triola, D. M. Badiane, A. V. Balatsky, and E. Rossi, *Phys. Rev. Lett.* **116**, 257001 (2016).
- [33] J. D. Sau and E. Demler, *Phys. Rev. B* **88**, 205402 (2013).
- [34] A. P. Mackenzie and Y. Maeno, *Rev. Mod. Phys.* **75**, 657 (2003).
- [35] A similar asymmetry for the energy of bound states with respect to $u_{\text{imp}} = 0$ has also been found for the case of d-wave superconductors [51]: also in that case such asymmetry is due to the dependence of the DOS on the energy.
- [36] T. Hyart, B. van Heck, I. C. Fulga, M. Burrello, A. R. Akhmerov, and C. W. J. Beenakker, *Phys. Rev. B* **88**, 035121 (2013), [arXiv:1303.4379](#).
- [37] D. Aasen, M. Hell, R. V. Mishmash, A. Higginbotham, J. Danon, M. Leijnse, T. S. Jespersen, J. A. Folk, C. M. Marcus, K. Flensberg, and J. Alicea, *Phys. Rev. X* **6**, 031016 (2016).
- [38] S. Plugge, A. Rasmussen, R. Egger, and K. Flensberg, *New Journal of Physics* **19**, 012001 (2017), [arXiv:1609.01697 \[cond-mat.mes-hall\]](#).
- [39] T. Karzig, C. Knapp, R. Lutchyn, P. Bonderson, M. Hastings, C. Nayak, J. Alicea, K. Flensberg, S. Plugge, Y. Oreg, C. Marcus, and M. H. Freedman, ArXiv e-prints (2016), [arXiv:1610.05289 \[cond-mat.mes-hall\]](#).
- [40] S. Vaitiekėnas, M. T. Deng, J. Nygård, P. Krogstrup, and C. M. Marcus, ArXiv e-prints (2017), [arXiv:1710.04300 \[cond-mat.mes-hall\]](#).
- [41] A. C. Potter and P. A. Lee, *Phys. Rev. B* **83**, 184520 (2011), [arXiv:1103.2129 \[cond-mat.supr-con\]](#).
- [42] A. C. Potter and P. A. Lee, *Phys. Rev. B* **84**, 059906 (2011), [arXiv:1108.2260 \[cond-mat.mes-hall\]](#).
- [43] A. M. Lobos, R. M. Lutchyn, and S. Das Sarma, *Phys. Rev. Lett.* **109**, 146403 (2012).
- [44] R. M. Lutchyn, T. D. Stanescu, and S. Das Sarma, *Phys. Rev. B* **85**, 140513 (2012), [arXiv:1110.5643 \[cond-mat.supr-con\]](#).
- [45] J. D. Sau, S. Tewari, and S. Das Sarma, *Phys. Rev. B* **85**, 064512 (2012), [arXiv:1111.2054 \[cond-mat.supr-con\]](#).
- [46] G. Tkachov, *Phys. Rev. B* **87**, 245422 (2013), [arXiv:1304.0631 \[cond-mat.mes-hall\]](#).
- [47] J. D. Sau and S. Das Sarma, *Phys. Rev. B* **88**, 064506 (2013), [arXiv:1305.0554 \[cond-mat.mes-hall\]](#).
- [48] H.-Y. Hui, J. D. Sau, and S. Das Sarma, *Phys. Rev. B* **92**, 174512 (2015), [arXiv:1508.04134 \[cond-mat.mes-hall\]](#).
- [49] W. S. Cole, J. D. Sau, and S. Das Sarma, *Phys. Rev. B* **94**, 140505 (2016), [arXiv:1603.03780 \[cond-mat.supr-con\]](#).
- [50] C.-X. Liu, J. D. Sau, T. D. Stanescu, and S. Das Sarma, ArXiv e-prints (2017), [arXiv:1705.02035 \[cond-mat.mes-hall\]](#).
- [51] W. A. Atkinson, P. J. Hirschfeld, A. H. MacDonald, and K. Ziegler, *Phys. Rev. Lett.* **85**, 3926 (2000).